JVSTB Journal of Vacuum Science & Technology B

Effects of doping type and concentration on precipitation of nanometer arsenic clusters in low-temperature-grown GaAs

W. N. Lee, Y. F. Chen, J. H. Huang, X. J. Guo, and C. T. Kuo

Citation: Journal of Vacuum Science & Technology B **23**, 2514 (2005); doi: 10.1116/1.2131872
View online: http://dx.doi.org/10.1116/1.2131872
View Table of Contents: http://scitation.aip.org/content/avs/journal/jvstb/23/6?ver=pdfcov
Published by the AVS: Science & Technology of Materials, Interfaces, and Processing

Effects of doping type and concentration on precipitation of nanometer arsenic clusters in low-temperature-grown GaAs

W. N. Lee[a)]
Department of Materials Science and Engineering, National Chiao Tung University, Hsinchu 300, Taiwan

Y. F. Chen and J. H. Huang[b)]
Department of Materials Science and Engineering, Materials Science Center, National Tsing Hua University, Hsinchu 300, Taiwan

X. J. Guo
Institute of Physics, Academia Sinica, Taipei 11529, Taiwan

C. T. Kuo
Department of Materials Science and Engineering, National Chiao Tung University, Hsinchu 300, Taiwan

(Received 27 April 2005; accepted 10 October 2005; published 11 November 2005)

In this study, the effects of doping type and concentration on arsenic precipitation in low-temperature-grown GaAs upon postgrowth annealing at 600, 700, and 800 °C were investigated. Three undoped/Si-doped/undoped (*i*-*n*-*i*) regions and three undoped/Be-doped/undoped (*i*-*p*-*i*) regions were grown by low-temperature molecular beam epitaxy. The results show that arsenic precipitation is dependent on doping type and doping concentration. Arsenic depletion was observed in all Be-doped layers for all annealing temperatures. However, a "dual" arsenic precipitation behavior was observed in Si-doped layers: As accumulates in $[Si]=2\times10^{18}$ cm^{-3} doped layers, while it depletes in $[Si]=2\times10^{16}$ and 2×10^{17} cm^{-3} doped layers. We attribute this "dual" As precipitation phenomenon in Si-doped layers to the different depletion depths. © *2005 American Vacuum Society.* [DOI: 10.1116/1.2131872]

I. INTRODUCTION

GaAs and related compounds grown by low-temperature molecular-beam epitaxy (LT-MBE) have attracted much attention due to their unique electronic and optical properties.[1–3] When grown at 200–300 °C, the LT-GaAs layers are very nonstoichiometric, containing about 1 at. % excess As and a high concentration of As related defects.[4] Upon postgrowth annealing above 500 °C, the excess As precipitate into clusters[5] and the LT layer's resistance changes to an extremely high-resistivity state ($>10^6$ Ω-cm).[6] This property offers the benefits of excellent device isolation in integrated circuits for the elimination of sidegating or backgating effects.[3] The reduced recombination time of about 400 fs[7,8] makes LT GaAs very suitable for ultrafast optoelectronic applications.

Although the annealed LT GaAs has demonstrated successful device applications, the out diffusion of As precipitates during annealing remains a major constraint in device design. It is, therefore, very important to control the density and distribution of As precipitates for potential device applications. Previous studies showed that As precipitation in annealed LT materials can be controlled by doping effects.[5,8–15] It has been found that As precipitates preferentially form in Si-doped GaAs then intrinsic and least favorably in Be-doped GaAs for moderately doped GaAs. However, when the Si and Be doping concentrations reach certain levels ($\geqslant5\times10^{18}$ cm^{-3}), an opposite precipitation behavior occurs.[9,16] Chang *et al.*[13] examined the As precipitation in an n-p_1-n-p_2-n-p_3 or an i-n_1-i-n_2-i-n_3-i structure, where "*i*," "*n*," and "*p*" denotes undoped, Si-doped, and Be-doped GaAs, respectively, with doping levels ranging from 2×10^{18} (n_1 or p_1) to 2×10^{16} cm^{-3} (n_3 or p_3). Upon postgrowth annealing at 800 °C, distinctive depletion zones could be observed along the i-n_1 interface, as generally expected. However, the depletion zone was less well defined or even unrecognizable at the i-n_2 and i-n_3 interfaces, and depletion zones along the p_1-n interface were narrower than those at the p_2-n and p_3-n interfaces; these precipitation behaviors can not be fully explained by the so-called "doping" or "Fermi-level" effect. Both the inter-diffusion of As related defects and doping effects during annealing among the LT layers make this a more complicated system for understanding the As precipitation behavior in lightly-doped LT GaAs. Thereby, in this study we designed a LT-GaAs structure consisting of three *i*-*n*-*i* and three *i*-*p*-*i* active regions, with doping levels ranging from 10^{16} to 10^{18} cm^{-3}, in which each active region is separated with a 10 nm AlAs marker layer. Owing to the high activation energy but small diffusion constant for Al and Ga inter-diffusion,[17] the thin AlAs layer also acts as an inter-diffusion barrier between adjacent active regions. By this way, the dependence of doping type and concentration on As precipitation behavior can be clearly distinguished. The As precipitation behavior was carefully characterized by transmission electron microscopy (TEM) and discussed.

a)Also with: Materials Science Center, National Tsing Hua University, Hsinchu 300, Taiwan; electronic mail: wnlee@mx.nthu.edu.twt
b)Electronic mail: jihhuang@mx.nthu.edu.tw

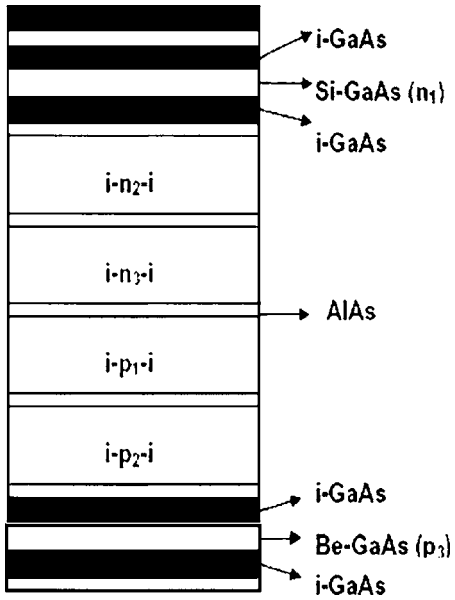

FIG. 1. Schematic of the LT-GaAs structure containing six active regions (i-n_1-i, i-n_2-i, i-n_3-i, i-p_1-i, i-p_2-i, and i-p_3-i multilayers). The "i" denotes 35 nm thick undoped GaAs layer, "n_1," "n_2," and "n_3" ("p_1," "p_2," and "p_3") denote the Si-doped (Be-doped) GaAs layers with doping concentration of 10^{16}, 10^{17}, and 10^{18} cm^{-3}, respectively. Each active region was separated by a 10 nm AlAs layer.

II. EXPERIMENT

The samples used in this study were grown by a Varian Modular GEN-II MBE system. The growth rates of 0.8 μm/h for GaAs and 0.2 μm/h for AlAs and the V/III beam equivalent pressure (BEP) ratio of 25 were used. Following native oxide desorption, a 100 nm GaAs buffer layer was first grown at 580 °C to smooth the surface, followed by a 10 nm AlAs diffusion barrier at the same temperature. Growth was then interrupted by closing the Al effusion furnace shutter, the substrate temperature was ramped down to 250 °C and the As shutter was closed when the substrate temperature was below 400 °C to maintain a clear 2×4 surface reconstruction, as observed by reflection high-energy electron diffraction (RHEED). It took about 15 min to stabilize the substrate temperature. Subsequently, the low-temperature active layers and a 35 nm GaAs cap layer were grown. As shown in Fig. 1, the LT-GaAs sample consisted of six active regions, i.e., three regions of undoped/Be-doped/undoped (i-p-i) multilayers and another three regions of undoped/Si-doped/undoped (i-n-i) multilayers. Each i-n-i or i-p-i region was separated by a thin AlAs layer, which acted as both a diffusion barrier and a marker layer. The thickness of each doped or undoped GaAs layer was 35 nm. The doping levels in the p_1,p_2, and p_3 layers (and n_1,n_2, and n_3 layers) were 2×10^{16}, 2×10^{17}, and 2×10^{18} cm^{-3}, respectively.

Postgrowth annealing was carried out in a rapid thermal annealing (RTA) system in forming gas ambient with a GaAs proximity cap at 600, 700 and 800 °C for 30 s. Arsenic precipitation in annealed samples was examined using a JEOL JEM-2010 transmission electron microscope. Cross-sectional samples parallel to (110) planes were prepared conventionally by mechanical thinning and Ar-ion milling. To further characterize the concentration of excess As incorporated into the LT-GaAs layers, three 1 μm thick LT GaAs control samples [Si]$=10^{18}$ cm^{-3} doped, [Be]$=10^{18}$ cm^{-3} doped, and undoped were also grown under the same growth conditions as aforementioned. Double-crystal x-ray diffraction (DXRD) rocking curves were examined using a Philip DCD-3 double-crystal diffractometer.

III. RESULTS AND DISCUSSION

Figures 2(a)–2(c) show the bright-field TEM images of six active regions after 30 s anneals at 600, 700, and 800 °C, respectively. The bright stripes seen in each picture are the AlAs layers. It is noted that AlAs layers provide good markers among the (i-n-i) or (i-p-i) regions. As precipitation depletion was observed in all Be-doped layers for all annealing temperatures; moreover, the As clusters accumulate toward the undoped layers. The DXRD rocking curves of GaAs (400) reflection for the three control samples are shown in Fig. 3. Clearly, peak separations of 108 and 72 arc s, caused by excess As incorporated in LT GaAs, were observed in Be-doped and undoped LT-GaAs epilayers, respectively; however, no obvious peak separation was observed in the Si-doped LT GaAs. This suggests that the Be doping enhanced the incorporation of excess As into the lattice of LT GaAs while the Si doping suppressed this effect. According to a previous report,[11] the concentration of As antisites, [As_{Ga}], is directly proportional to the lattice expansion of the LT-GaAs epilayer. Therefore, we can conclude that $[As_{Ga}]_{p3}>[As_{Ga}]_i>[As_{Ga}]_{n3}$, where $[As_{Ga}]_x$ denotes the As antisite concentration in the x-doped control sample. Moreover, during postgrowth annealing, the reduction of strain caused by the As_{Ga} defects is also a driving force for precipitation. For the i-p_3-i region, the As_{Ga} defects diffused from the p_3 to i layers, and for the i-n_3-i region from i to n_3 layer, which is opposite to the V_{Ga} defects. Our experimental result about i-n_3-i region and all i-p-i regions is therefore consistent with the vacancy-assisted As antisite diffusion mechanism.[8,10,12,13]

Interestingly, we observed a "dual" As precipitation phenomenon[9] in Si-doped regions: As precipitates accumulate toward the center of the [Si]$=2\times10^{18}$ cm^{-3} doped layer for all annealed temperatures; however, As precipitates are depleted away the other two lightly Si-doped regions ($n=2\times10^{16}$ and 2×10^{17} cm^{-3}) toward the undoped regions. The latter depletion behavior contrasts with the earlier observation by Chang *et al.*[13] In their work, the i-n_1-i-n_2-i-n_3-i multiplayer structure did not consist of any isolation layer to prevent the inter-diffusion of defects and doping effect from n_1 to n_2 or n_3. As a result, As precipitation behaviors were disturbed and the correlation of doping concentration to As precipitation could not be clearly identified.

The "dual" As precipitation phenomenon in Si-doped GaAs layers indicates that other effects must be considered in addition to the vacancy-assisted As antisite diffusion mechanism. According to the analysis of O'Hagan *et al.*,[16]

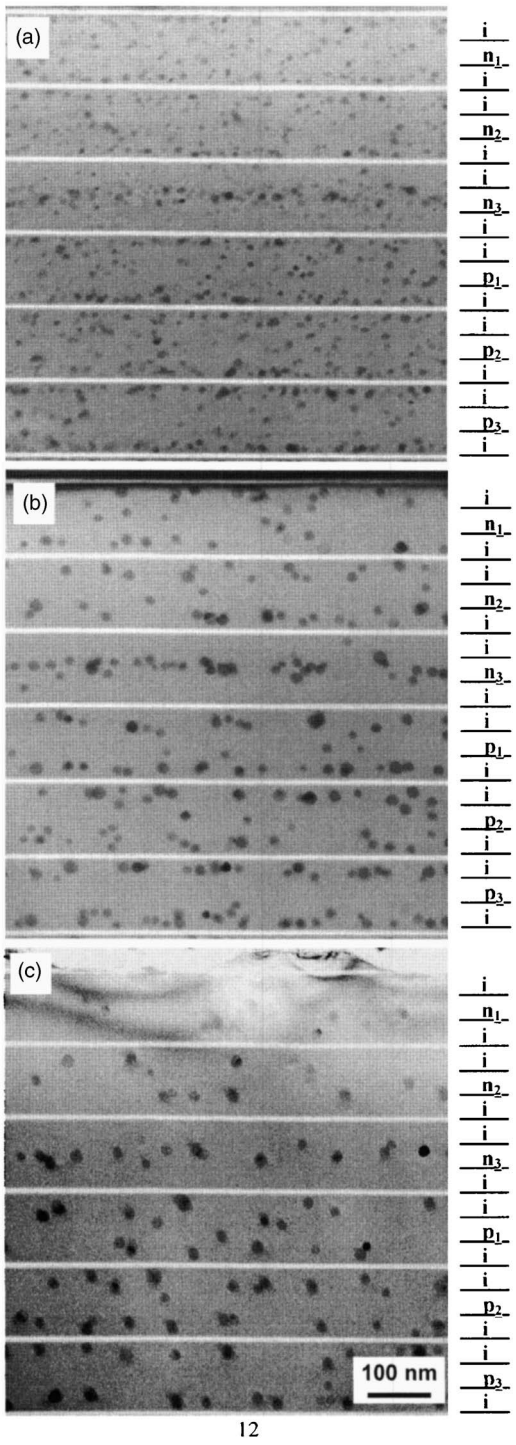

FIG. 2. TEM bright field images showing arsenic precipitates in different active regions after annealing at (a) 600, (b) 700, and (c) 800 °C, respectively.

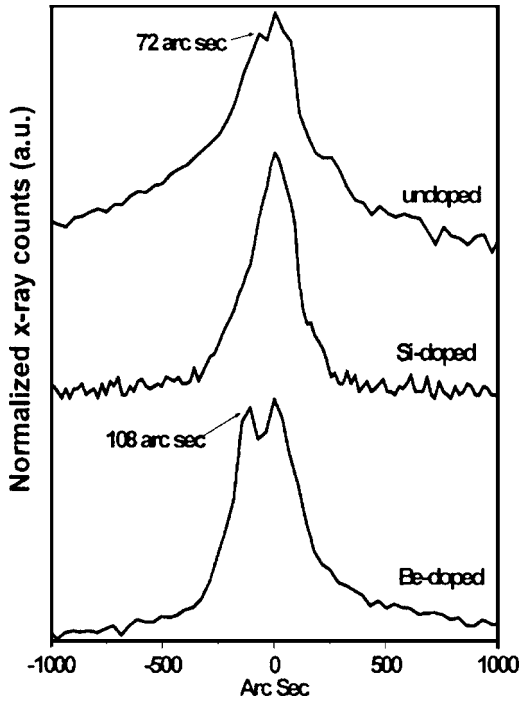

FIG. 3. DXRD rocking curves of GaAs (400) for 1 μm thick undoped, $[Si]=10^{18}$ cm^{-3} doped, and $[Be]=10^{18}$ cm^{-3} doped LT GaAs control samples.

As precipitation at the i/n interface can be influenced by the Debye length,[18] $\lambda_D=\{\varepsilon\varepsilon_0 kT/[q^2(N_D-N_A)]\}^{1/2}$. Following this argument, band bending[14,18,19] and depletion of the "n" regions to a depth of up to a few Debye lengths would occur at each i/n interface. Moreover, according to the model proposed by Chandra *et al.*,[18] the Debye lengths at the current annealing temperatures in our structure are estimated to be around 560, 180, and 50 Å for n_1, n_2, and n_3 layers, respectively. Therefore, the total depletion depth should be $\sim$1120, $\sim$360, and $\sim$100 Å for n_1, n_2, and n_3 layers, respectively, due to the double n/i interfaces in each active region. Therefore, since each Si-doped layer is 350 Å thick, it is likely that complete depletion occurred in the n_1 and n_2 layers but an incomplete depletion in the n_3 layer, the latter was also noted as an "As accumulation" layer.

Figure 4 shows the average density of As clusters in each *i-x-i* region after annealing at 700 and 800 °C, respectively. The density of As clusters was determined by assuming that the sample thickness under TEM investigation was 100 nm. The analysis reveals that the cluster densities of the *i-p-i*

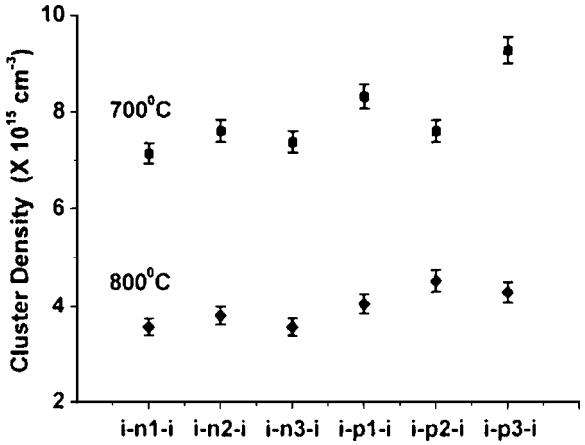

FIG. 4. As cluster density in each *i-x-i* region after annealing at 700 and 800 °C, where $x=n_i$ or p_i.

regions are higher than those of the *i-n-i* regions under the same doping concentration and annealing condition, which is consistent with the DXRD results.

IV. CONCLUSION

The effect of doping type and concentration on As precipitation in LT-GaAs upon post-growth annealing at 600, 700, and 800 °C was investigated. The results show that the As precipitation is dependent on doping type and doping concentration. As depletion were observed in all Be-doped regions. However, a "dual" arsenic precipitation phenomenon was observed in Si-doped regions: As precipitation accumulation was observed in $[Si]=2\times10^{18}$ cm^{-3} doped layer for all annealing temperatures, while As precipitation depletion was observed in $[Si]=2\times10^{16}$ and 2×10^{17} cm^{-3} doped layers. The "dual" arsenic precipitation phenomenon in Si-doped layers can be attributed to the different depletion depths caused by various doping concentrations.

ACKNOWLEDGMENTS

This work was supported by the National Science Council, Republic of China, under Contract Nos. NSC 92-2112-M-007-032 and NSC 92-2120-M-007-006.

[1]D. C. Look and D. C. Walters, Phys. Rev. B **42**, 3578 (1990).
[2]D. D. Nolte, M. R. Melloch, J. M. Woodall, and S. J. Ralph, Appl. Phys. Lett. **62**, 1356 (1993).
[3]F. W. Smith, A. R. Calawa, C.-L. Chen, M. J. Manfra, and L. J. Mahoney, IEEE Electron Device Lett. **9**, 77 (1988).
[4]T. J. Rogers, C. Lei, B. G. Streetman, and D. G. Deppe, J. Vac. Sci. Technol. B **11**, 926 (1993).
[5]M. R. Melloch, N. Otsuka, K. Mahalingam, P. D. Kirchner, J. M. Woodall, and A. C. Warren, Appl. Phys. Lett. **61**, 177 (1992).
[6]A. C. Warren, J. M. Woodwall, J. L. Freeouf, D. Grischkowsky, D. T. McInturff, M. R. Melloch, and N. Otsuka, Appl. Phys. Lett. **57**, 1331 (1990).
[7]S. Gupta, M. Y. Frankel, J. A. Valdmanis, J. F. Whitaker, G. A. Mourou, F. W. Smith, and A. R. Calawa, Appl. Phys. Lett. **59**, 3276 (1991).
[8]D. E. Bliss, W. Walukiewicz, J. W. Ager, III, E. E. Haller, K. T. Chan, and S. Tanigawa, J. Appl. Phys. **71**, 1699 (1992).
[9]J. H. Huang, L. Z. Hsieh, X. J. Guo, and Y. O. Su, Appl. Phys. Lett. **82**, 305 (2003).
[10]M. R. Melloch, N. Otsuka, K. Mahalingam, C. L. Chang, J. M Woodall, G. D. Pettit, P. D. Kirchner, F. Cardone, A. C. Warren, and D. D. Nolte, J. Appl. Phys. **72**, 3509 (1992).
[11]X. Liu, A. Prasad, J. Nishio, E. R. Weber, Z. Liliental-Weber, and W. Walukiewicz, Appl. Phys. Lett. **67**, 279 (1995).
[12]M. N. Chang, J.-W. Pan, J.-I. Chyi, K. C. Hsieh, and T.-E. Nee, Appl. Phys. Lett. **72**, 587 (1998).
[13]M. N. Chang, K. C. Hsieh, T.-E. Nee, and J.-I. Chyi, J. Appl. Phys. **86**, 2442 (1999).
[14]M. Missous and S. O'Hagan, J. Appl. Phys. **75**, 3396 (1994).
[15]T. M. Cheng, C. Y. Chang, and J. H. Huang, Jpn. J. Appl. Phys., Part 1 **34**, 1185 (1995).
[16]S. P. O'Hagan, M. Missous, A. Mottram, and A. C. Wright, J. Appl. Phys. **79**, 8384 (1996).
[17]L. L. Chang and A. Koma, Appl. Phys. Lett. **29**, 138 (1976).
[18]A. Chandra, C. E. C. Wood, D. W. Woodard, and L. F. Eastman, Solid-State Electron. **22**, 645 (1979).
[19]D. C. Look, D. C. Walters, M. Mier, C. E. Stutz, and S. K. Brierley, Appl. Phys. Lett. **60**, 2900 (1992).